Quinazoline-based analog of adenine as an antidote against MLL-rearranged leukemia cells: synthesis, inhibition assays and docking studies

Corentin Bon, Magdalena Barbachowska, Nemanja Djokovic, Dusan Ruzic, Yang Si, Laura Soresinetti, Corinne Jallet, Ambre Tafit, Ludovic Halby, Katarina Nikolic, et al.

Quinazoline-based analogue of adenine as an antiDOTe against MLLr cells: synthesis, inhibition assays and docking studies

Corentin Bon[1,2], Magdalena Barbachowska[1,2], Nemanja Djokovic[3], Dusan Ruzic[3], Yang Si[1], Laura Soresinetti[1], Corinne Jallet[1], Ambre Tafit[1], Ludovic Halby[1], Katarina Nikolic[3,] and Paola B. Arimondo [1,*]

[1]*Epigenetic Chemical Biology, Department of Structural Biology and Chemistry, Institut Pasteur, UMR3523 CNRS, 75015 Paris, France*

[2] *Ecole Doctorale MTCI, Université de Paris, Sorbonne Paris Cité, Paris, France*

[3] *Department of Pharmaceutical Chemistry, Faculty of Pharmacy, University of Belgrade, Vojvode Stepe 450, 11000 Belgrade, Serbia*

* Correspondence: should be addressed to Paola B. Arimondo, EpiCBio, Institut Pasteur, CNRS UMR3523, email: paola.arimondo@cnrs.fr

Running title: Synthesis of a quinazoline-based DOT1L inhibitor

Abstract

Background. Post-translational modifications of histones constitute a dynamic process impacting gene expression. A well-studied modification is lysine methylation. Among the lysine histone methyltransferases, DOT1L is implicated in various diseases making it a very interesting target for drug discovery. DOT1L has two substrates, the SAM cofactor that gives the methyl group and the lysine H3K79 substrate.

Results. Using molecular docking we explored new bisubstrate analogues to enlarge the chemical landscape of DOT1L inhibitors. We showed that quinazoline can successfully replace the adenine in the design of bisubstrate inhibitors of DOT1L, showing a similar activity compared to the adenine derivative but with a diminished cytotoxicity.

Conclusions. The docking model is validated together as the use of quinazoline in the design of bisubstrate inhibitors.

Keywords: adenine analogues, bisubstrate inhibitors, chemical probes, Epigenetics, DOT1L, MLLr leukaemia

Introduction

Conrad H. Waddington defined Epigenetics in 1942 as the study of phenotypic changes without modification of the genotype[1]. Since then, the definition has evolved continuously with the understanding of the complexity of the mechanisms involved and the advances in the field [2–4]. Currently, Epigenetics is defined as the modulations of gene expression that do not involve DNA sequence alteration, in particular through reversible and transmissible chemical changes [5],[6]. This dynamics is linked to three major protein families responsible either for the introduction of the epigenetic chemical modifications ("writers"), for their recognition ("readers") or their removal ("erasers"). Among the writers, the histone methyltransferases (HMT) [7] catalyse the methylation of lysines and arginines of histones by transfer of a methyl group from the *S*-adenosyl-L-methionine (SAM) cofactor to the substrate. This reaction can lead to mono-, di- and tri-methylation of lysines, and monomethylation and dimethylation, either symmetrically or asymmetrically, of arginines[8]. To date, the most studied is the methylation of lysine 4 (H3K4), lysine 9 (H3K9), 27 (H3K27), 36 (H3K36), 79 (H3K79) of histone 3 and lysine 20 (H4K20) of histone 4. Depending on the methylated lysine and the level of methylation, these modifications induce the formation of euchromatin or heterochromatin and can either activate or repress expression of genes [9].

Deregulation of histone methylation is associated with cancer and other pathologies [10],[11],[12] and constitutes a promising therapeutic targets. The first inhibitor of a lysine histone methyltransferase (KMT), Tazemetostat™, targeting the enzyme EZH2, has been by Food and Drug Administration (FDA) approved in 2020 to treat advanced epithelioid sarcoma and follicular lymphoma [13–15]. Thus, there is a great interest in finding new chemical scaffold that inhibit KMTs. Bisubstrate inhibitors are a promising strategy as KMT have two substrates, the SAM, the methyl donor, and the lysine that will be

methylated [16] . Bisubstrate analogues are designed by covalent coupling of mimics of each substrate.

Among the KMTs, DOT1L (DOT1-Like) plays a particular role as it is the only methyltransferase that catalyses the mono-, di- and trimethylation of lysine 79 of histone H3[17]. Deregulation of H3K79 methylation catalysed by DOT1L results in aberrant transcriptional activation ~~is~~ implicated in the development of MLL rearranged leukaemia (MLLr). Oncogenic chromosomal rearrangements of the MLL gene are involved in the aberrant recruitment of DOT1L activity[18]. Inhibition of DOT1L activity or disruption of the interaction between DOT1L with MLL fusion partners[19,20] are potential therapeutic strategies for the treatment of MLLr[21],[22,23], along with other paediatric AML leukaemia[24]. Several adenosyl-based compounds were discovered[25,26] that behave as bisubstrate analogues. Pinometostat (EPZ-5676) reached phase 1/2 clinical trials[27], but it showed poor pharmacological properties [28]. We and others synthesised analogues to improve the metabolic stability [26,29–31]. Here, we describe the use of the quinazoline moiety as adenine isostere to enlarge the chemical variety and the design of a new bisubstrate inhibitor of DOT1L. We developed a docking model to select by virtual screening the potential bisubstrate inhibitors to synthetize. This strategy has been shown to be efficient in the past[32] and allowed to focus our chemistry efforts on the most promising structures. The synthetised compounds were then tested for their ability to inhibit DOT1L enzymatic activity *in vitro* and their effect on the proliferation of MLLr cells. The results show that the quinazoline scaffold can successfully replace the adenine moiety in the design of bisubstrates inhibitors of DOT1L with a comparable activity *in vitro* and in cells but with a lower cytotoxicity.

Materials and Methods

Chemical synthesis

All chemicals were purchased from Sigma-Aldrich, Alfa Aesar, Carbosynth and FluoChem. As described previously by us [26] NMR experiments were recorded on an Agilent DirectDrive 500 spectrometer (Agilent Technologies, Santa Clara) with a proton resonating frequency of 499.8 MHz~~. Spectra were recorded~~ using the VnmrJ 4.2A software (Agilent Technologies). Chemical shifts are given in ppm, coupling constants *J* in Hz. Splitting patterns are as follows: s, singlet; bs broad singlet; d, doublet; bd broad doublet; t, triplet; brt, broad triplet; dd, doublet of a doublet; m, multiplet; ddd, doublet of a doublet of a doublet; q, quartet; quint, quintet. MS-ESI were performed on a Bruker MicroTOF and HRMS analyses on a Q Exactive mass Spectrometer (Thermofisher). Samples were previously dissolved in a mix of water and acetonitrile (50/50) and 0.1% of formic acid. Full scans (150-2000Da) were acquired in positive ion mode with a resolution of 70,000.

Di-*tert*-Butyl (4,5-dihydroxycyclopentane-1,3-diyl)dicarbamate (6)

To a solution of (1*R*,2*S*,3*R*,5*S*)-3,5-diaminocyclopentane-1,2-diol[33] (1.3g, 10mmol) in 50mL dioxane and 20mL of a 1M K_2CO_3 solution was added Boc_2O (2.5g, 11mmol) and stirred at RT overnight. Dioxane was evaporated and the aqueous phase extracted with ethyl acetate four times. The combined organic phases were dried with brine and over Na_2SO_4. The solvents were removed under vacuum to obtain **6** (3.2g, 9.5mmol, 95%) as a white powder without any further purification.

HRMS-ESI(m/z) calculated for $C_{15}H_{28}N_20_6$ $[M+H]^+$: 333.2020 ; Found: 333.2017.

^{1}H NMR (500 MHz, DMSO-*d6*) δ 6.75 (d, *J* = 7.9 Hz, 2H), 4.61 – 4.56 (m, 2H), 3.59 (dt, *J* = 16.5, 5.9 Hz, 4H), 2.30 (dt, *J* = 13.5, 8.4 Hz, 1H), 1.39 (s, 18H), 1.06 (dt, *J* =

13.2, 6.4 Hz, 1H).

^{13}C NMR (126 MHz, DMSO-*d6*) δ 155.4, 78.0, 75.7, 54.5, 40.2, 28.7.

Di-*tert*-Butyl (2,2-dimethyltetrahydro-4H-cyclopenta[d][1,3]dioxole-4,6-diyl)dicarbamate (7)

To a solution of **6** (3.2g, 9.5mmol) in 100mL of dry acetone was added 2,2-dimethoxypropane (18mL, 15mmol) and APTS (86mg, 0.5mmol). The mixture was stirred at RT under argon for 16h. Acetone was evaporated and the residual oil diluted with ether and washed with water . The organic phase was dried over Na_2SO_4 and solvents were evaporated to yield **7** (3.4g, 9.2mmol, 96%) as a white powder.

HRMS-ESI(m/z) calculated for $C_{18}H_{32}N_2O_6$ $[M+H]^+$: 373.2333 ; Found: 373.2321

^{1}H NMR (500 MHz, Chloroform-*d*) δ 4.87 – 4.82 (m, 2H), 4.56 (s, 2H), 3.93 (dt, *J* = 6.6, 4.1 Hz, 2H), 2.49 (dt, *J* = 14.1, 7.0 Hz, 1H), 1.74 (dt, *J* = 14.1, 4.1 Hz, 1H), 1.61 (s, 3H), 1.48 (s, 18H), 1.30 (s, 3H).

^{13}C NMR (126 MHz, $CDCl_3$) δ 155.3, 111.3, 85.4, 80.0, 77.2, 57.4, 35.9, 28.3, 26.7, 24.4.

2,2-Dimethyltetrahydro-4H-cyclopenta[d][1,3]dioxole-4,6-diamine (8)

To a solution of **7** (1.8g, 5mmol) in 20mL of dry DCM under argon was added 5mL of TFA and the mixture was stirred at RT for 1h. The solvents were removed under vacuum and the residual oil co-evaporated with a 7M ammonia solution in methanol twice. The residue was purified by flash chromatography using a linear gradient of a solution of 0.1N ammonia in methanol (0 to 10 %) in DCM. Compound **8** (650mg, 3.79mmol, 75%) was obtained as a white hygroscopic powder.

HRMS-ESI(m/z) calculated for $C_8H_{16}N_2O_2$ $[M+H]^+$: 173.1282 ; Found: 173.1279

^{1}H NMR (500 MHz, Chloroform-*d*) δ 6.95 (m, 2H), 4.77 – 4.72 (m, 2H), 4.34 (s, 2H), 3.93 (m, 2H), 2.34 (m, 1H), 1.74 (m, 1H), 1.64 (s, 3H), 1.29 (s, *J* = 0.8 Hz, 3H).

^{13}C NMR (126 MHz, $CDCl_3$) δ 110.7, 87.5, 38.8, 26.6, 24.3.

4-(1H-1,2,4-Triazol-1-yl)quinazoline (9)

To a solution of 1,2,4-triazol (14.0g; 203mmol) in 100 mL acetonitrile at 0°C, $POCl_3$ (6.0mL, 152.7mmol) was added. TEA (28mL, 200mmol) was then added dropwise. The reaction mixture was stirred at 0°C for 30min, then at RT for another 30min. 4-hydroxyquinazoline (3.2g, 22 mmol) was added and the heterogeneous mixture stirred at RT overnight. The mixture was finally refluxed for 2h, cooled to RT then diluted with ice water (100mL) and stirred at 0°C for 15min. The suspension was filtrated and the solid was washed with water 3 times and with a minimum amount of ethanol to yield **9** (3.2g, 1.62mmol, 74%) as a white powder. The product was used without further purification.

HRMS-ESI(m/z) calculated for $C_{10}H_7N_5$ $[M+H]^+$: 198.0774 ; Found: 198.0759

1H NMR (500 MHz, DMSO-*d6*) δ 9.61 (s, 1H), 9.24 (s, 1H), 9.06 (dt, *J* = 8.7, 1.1 Hz, 1H), 8.54 (s, 1H), 8.14 – 8.09 (m, 2H), 7.86 (m, 1H).

^{13}C NMR (126 MHz, DMSO-*d6*) δ 157.2, 156.6, 155.8, 149.0, 138.3, 132.3, 131.4, 129.4, 119.0.

(±) 2,3-*O*-Isopropyliden-(1ß,2α,3α,5β)-3-amino-5-(quinazolin-4-ylamino)cyclopentanediol (**10**)

To a solution of **8** (860mg, 5.0mmol) and triethylamine (1.5mL, 11mmol) in 20 mL of

acetonitrile, a solution of **9** (950mg, 4.8mmol) in 10mL of acetonitrile was added dropwise. The mixture was stirred at RT overnight, then the solvent removed under vacuum. The residue was purified by flash chromatography using a linear gradient of a solution of 0.1N ammonia in methanol (0 to 10 %) in DCM, yielding **10** (1.1g, 3.65 mmol, 74%) as a white powder.

HRMS-ESI(m/z) calculated for $C_{16}H_{20}N_4O_2$ $[M+H]^+$: 300.1586 ; Found: 300.1569

^{1}H NMR (500 MHz, DMSO-*d6*) δ 8.61 (s, 1H), 8.34 (dd, *J* = 8.4, 1.3 Hz, 1H), 7.86 (dddd, *J* = 11.5, 8.3, 7.0, 1.3 Hz, 1H), 7.74 (dt, *J* = 8.4, 1.7 Hz, 1H), 7.63 – 7.56 (m, 1H), 4.88 (dd, *J* = 7.2, 4.6 Hz, 1H), 4.66 (ddd, *J* = 10.3, 6.8, 4.5 Hz, 2H), 3.56 (ddd, *J* = 10.6, 6.7, 4.6 Hz, 1H), 2.62 – 2.52 (m, 1H), 1.97 (dt, *J* = 12.9, 9.8 Hz, 1H), 1.46 (s, 2H), 1.25 (s, 3H).

^{13}C NMR (126 MHz, DMSO-*d6*) δ 162.6, 161.2, 156.9, 136.8, 129.6, 126.4, 121.5, 119.1, 117.4, 86.0, 84.5, 58.6, 57.3, 30.1, 28.0.

General procedure for compounds 1 and 2

A mixture of amine **3** or **10** (1eq) and 3-[2-(5-*tert*-butyl-1*H*-1,3-benzodiazol-2-yl)ethyl]cyclobutan-1-one hydrochloride[34](2 eq) and triethylamine (1eq) in methanol was stirred at RT for 2h. $NaBH(OAc)_3$ (5eq) and AcOH (1.05eq) were added. After 12h, the solvent was evaporated. TFA was added along with 1eq of water and the mixture was stirred at RT for 1h, the volatiles were evaporated and the crude purified on reverse phase AQ chromatography using a linear gradient of 0 to 100% acetonitrile with 0.1% formic acid in a 0.1% formic acid solution as eluent to obtain compound **1** and a linear gradient of 0 to 100% acetonitrile with 0.01% TEA in a 0.01% TEA solution as eluent to obtain compound **2**.

(1*R*,2*S*,3*R*,5*S*)-3-(6-amino-9*H*-purin-9-yl)-5-((3-((5-(*tert*-butyl)-1H-benzo[*d*]imidazol-2-yl)methyl)cyclobutyl)amino)cyclopentane-1,2-diol (**1**)

(17mg, 0.034 mmol 47%)

HRMS-ESI(m/z) calculated for $C_{27}H_{37}N_8O_2$ $[M+H]^+$: 505.2961; Found: 505.3041.

^{1}H NMR (500 MHz, DMSO-*d6*) δ 8.19 – 8.11 (m, 3H), 7.61 – 7.53 (m, 2H), 7.46 – 7.39 (m, 1H), 7.35 (s, 2H), 5.47 (s, 2H), 4.72 – 4.63 (m, 1H), 4.47 – 4.39 (m, 1H), 4.20 – 4.12 (m, 1H), 3.68 (p, *J* = 8.3 Hz, 1H), 3.35 – 3.25 (m, 1H), 2.98 – 2.89 (m, 2H), 2.63 – 2.51 (m, 1H), 2.42 – 2.29 (m, 2H), 2.26 – 2.15 (m, 1H), 2.02 (d, *J* = 17.7 Hz, 2H), 1.97 – 1.89 (m, 1H), 1.88 – 1.76 (m, 1H), 1.34 (s, 9H).

^{13}C NMR (126 MHz, DMSO-*d6)* δ 156.1, 154.1, 151.9, 149.2, 146.7, 140.3, 134.2, 132.4, 121.6, 119.4, 113.6, 109.8, 73.1, 71.5, 59.0, 58.5, 46.7, 34.7, 33.6, 32.1, 32.1, 31.5, 29.9, 29.8, 29.2, 27.6, 24.9.

(±) (1*β*,2*α*,3*α*,5*β*)-3-((3-(2-(5-(*tert*-butyl)-1*H*-benzo[*d*]imidazol-2-yl)ethyl)cyclobutyl)amino)-5-(quinazolin-4-ylamino)cyclopentane-1,2-diol (**2**)

(14mg, 0.027 mmol, 38%)

HRMS-ESI(m/z) calculated for $C_{30}H_{38}N_6O_2$ $[M+H]^+$: 514.3056; Found: 514.3113.

^{1}H NMR (500 MHz, DMSO-*d6*) δ 10.00 – 9.95 (m, 1H), 9.46 – 9.20 (m, 2H), 8.93 (s, 1H), 8.63 – 8.57 (m, 1H), 8.06 (ddd, *J* = 8.3, 7.1, 1.2 Hz, 1H), 7.85 (dd, *J* = 8.5, 1.2 Hz, 1H), 7.82 – 7.76 (m, 1H), 7.73 – 7.64 (m, 2H), 7.64 – 7.57 (m, 1H), 4.73 – 4.64 (m, 1H), 4.46 – 4.38 (m, 2H), 4.18 – 4.08 (m, 2H), 3.75 – 3.62 (m, 1H), 3.37 – 3.21 (m, 1H), 3.14 – 2.98 (m, 2H), 2.58 – 2.51 (m, 1H), 2.44 – 2.24 (m, 2H), 2.09 – 1.61 (m, 5H), 1.35 (s, 9H).

^{13}C NMR (126 MHz, DMSO-*d6*) δ 160.7, 153.9, 153.8, 151.3, 148.7, 138.1, 136.0, 131.2, 129.0, 128.3, 124.3, 123.5, 119.7, 113.3, 112.9, 109.6, 73.3, 72.0, 64.9, 58.9, 55.8, 46.7, 34.9, 33.0, 32.0 (d), 31.3, 29.9 (d), 29.3, 27.4, 23.9.

Molecular docking

The cocrystal structure of the DOT1L enzyme in complex with EPZ-5676 was acquired from Protein Data Bank (PDB code: 4HRA). The enzyme-inhibitor complex was pre-processed using *PlayMolecule* ProteinPrepare web application.[35] Structures of ligands were optimized with Hartree-Fock (HF) theory and 3-21G basis set, using Gaussian 09 software[36] implemented in ChemBio3D Ultra13.0 program.[37] The binding modes of the synthesized compounds (**1** and (±)-**2**) were examined by molecular docking using GOLD 5.8.1 software.[38] Studied ligands were docked into SAM binding pocket of DOT1L, defined as residues in 6Å radius of cocrystal ligand. The chemical bonds of ligands were enabled to rotate freely. Number of genetic algorithm runs were set on 30 and search efficacy was set to 200%. The GoldScore fitness function was used to rank the compounds' binding poses. To validate docking setup, RMSD value (root mean square deviation of atomic position) was used after redocking of co-crystal ligand. Obtained RMSD = 0.659Å qualified the procedure as accurate for predictions of structurally related ligands. Data visualization was performed in Pymol [39] and 2D interaction plots were generated using PoseView [40].

Biological essays

DOT1L enzymatic inhibition assays

The tests were carried out in 384-well white plates (Corning ref # CLS 3673) as

previously described[26]. Recombinant DOT1L protein (1-416aa) from Reaction Biology Corp (# HMT-11-101), non-recombinant and unmethylated oligonucleosomes (Reaction biology Corp # HMT-35-130) containing 50 additional base pairs of internucleosomal DNA purified from HeLa cells and poly-L-Lysine in the high salt buffer (50mM Tris-HCl pH 7.4, 1M NaCl, 0.1% Tween-20, 0.3% poly-L-Lysine) (P1399, Sigma Aldrich) were used. The SAM (Sigma-Aldrich ref # A70007) is aliquoted in water at – 80°C. Reactions were performed in the "Assay Buffer" (AB) (50mM Tris-HCl pH8, 150mM NaCl, 3mM $MgCl_2$, 0.1% BSA). Dilutions of protein, inhibitors and oligonucleosomes were prepared freshly in AB just before use. Briefly, the methylation reaction was performed in 384-well plate and initiated after 10min incubation of the compound with 80nM DOT1L enzyme. Then, 2µM of cofactor SAM and 0.5 ng of oligonucleosomes was added per well and incubated for 45min at RT. The reaction was stopped by addition of poly-L-lysine and incubation for 15min at RT. Anti-Histone H3 (C-ter) AlphaLISA acceptor beads (PerkinElmer, #AL147) (0.1mg/mL final) and AlphaLISA biotinylated anti-dimethyl-Histone H3 Lysine 79 (H3K79) antibody (PerkinElmer, #AL148) (5nM final) were mixed in the detection buffer (DB) (AlphaLISA 5X Epigenetics Buffer 1 + AlphaLISA 30X Epigenetics Buffer Supplement, PerkinElmer, #AL008C1 & #AL008C2) and added for 1h at RT. Then 5µL Alpha Streptavidin Donor beads (PerkinElmer, #6760002) (0.1mg/mL final) in DB was incubated for 30min at RT and the plates were read ~~using~~ on an EnVision 2103 multilabel plate reader (PerkinElmer) in AlphaLISA mode. Samples were run in technical triplicates. The percentage of inhibition was calculated as the mean of at least three experiments. The percentage inhibition was calculated using the following equation:

% of inhibition = $(1 - (\frac{Xi - Xm}{XM - Xm})) * 100;$

where Xi, Xm, XM are the average signal at the considered concentration, minimal signal response (without enzyme and compound) and maximum signal response (without compound), respectively. Data analysis was performed using the GraphPad Prism 5 software. IC_{50} values were determined using the nonlinear regression fittings with sigmoidal dose-response (variable slope) function and the displayed EC_{50} are the mean of three independent experiments with associated standard deviations.

Cell culture

Human leukaemia cell line MV4-11 (CRL-9591) was purchased from American Type Culture Collection (Manassas, VA). Cells were cultured in Roswell Park Memorial Institute (RPMI) 1640 Medium (RPMI) supplemented with 10 % Foetal Bovine Serum (FBS), 5% GlutaMAX ™ to prevent the accumulation of toxic ammonia and maintained in a humidified atmosphere at 37°C and 5 % CO_2. Cells were reseeded every 4 to 5 days to 0.5 million cells/mL. All cell culture reagents were purchased from Gibco ThermoFisher Scientific.

For assessment of cell proliferation and viability, exponentially growing MV4-11 cells were seeded in triplicate, in 96-well plates, at a density of 35000 cells/well in a final volume of 100µL. Cells were incubated in the presence of 1, 3.2 and 10 µM of compounds **1** or **(±)-2** and 0.1% of DMSO was used as a negative control. Viable cell number was determined every 3–4 days for up to 15 days to 21 days using blue trypan counting in Cellometer Disposable Counting Chambers and read on the Cellometer Mini Automated Cell Counter.

For cytotoxicity assays, MV4-11 cells (www.atcc.org) were treated with the test compound solutions at a dose range from 1 × 10−9 M to 32 × 10−5 M. On day 4 the antiproliferative activity of compounds was measured using the ATP quantification

method “ATPlite One Step Luminescence Assay System” (PerkinElmer) according to the manufacture instructions. Data were analysed with GraphPad Prism 5 software to evaluate the compound concentration required to cause a 50% decrease in cell viability as compared with untreated controls.

Histone Extraction

The experimental procedure was described by us in[26]. One to two million MV4-11 cells were harvested after 6 days treatment with increasing inhibitor concentrations (0.1, 0.32, 1, 3.2, 10 μM). Histones were extracted by centrifugation at 200g and lysed by 5min of incubation on ice in 250μL of nuclear extraction buffer (10mM Tris-HCl, 10mM $MgCl_2$, 25mM KCl, 1% Triton X-100, 8.6% sucrose, Roche Protease inhibitor tablet 1836145). The nuclei were collected by centrifugation at 600g for 5min at 4 °C. The supernatant was discarded and the histones were extracted with 0.4N cold sulfuric acid for 1h at 4°C. The extracts were centrifugated at 10,000g for 10min at 4 °C and transferred to a microcentrifuge tube containing 10x volume of ice-cold acetone. Histones were precipitated at -20 °C overnight and recovered by centrifugation at 1500g for 10min then resuspended in 80μL of water. Histones were quantified by the absorbance measured at 276 nm on a NanoDrop 2000.

Western Blotting

After extraction, histones (500 ng) were separated on 4%-20% Tris-Glycine gels (Invitrogen) and transferred onto a nitrocellulose membrane (0.2 mm) using the iBlot® Gel Transfer Stacks Nitrocellulose kit Mini (Invitrogen). After blocking nonspecific sites for 1h at RT in a solution of 1X TBS at 5% milk, the membrane was incubated with rabbit anti-H3K79me2 (ab3594, 1/1000) or anti-H3 (ab1791)1/1000) for 1h at RT. The

membrane was washed 3 times 5 minutes in a 1x TBS solution containing 0.05% Tween20 and then incubated with an HRP anti-rabbit secondary antibody (NA934V, 1/10000) for 1h at RT. The membrane was washed three times with TBST and was revealed using the ECL ™ Prime Western Blotting Detection Reagents Developer Kit (GE Healthcare).

Results and discussion

2.1. Chemical design

Compounds EPZ-4777 and EPZ-5676 (Figure 1) were developed by Epizyme as potent inhibitors of DOT1L with anti-tumour activity in MLLr cells lines and xenografts [27,41–43]. EPZ-5676 was the first HMT inhibitor to enter clinical trials for the treatment of adults and paediatric patients with relapsed/refractory MLLr leukaemia. A limitation to the activity of the compound is the poor pharmacological properties implying an administration by continuous IV infusion. In a previous study, we replaced with success the ribose sugar with a cyclopentane diol moiety in compound EPZ-4777, resulting in a nanomolar inhibitor of DOT1L (called Dia-2) with potent cellular activity[26]. Here, we kept the cyclopentanediol moiety and explored the possibility of replacing the adenine moiety mimicking the SAM substrate with different heterocycles. We designed a chemical library of 50 analogues of Dia2 [26] (Supplementary Table 1), in which the adenine moiety was replaced by a representative panel of heterocycles to cover the pharmacophores of the adenine (general structure in Supplementary Figure S3), including six and five member rings such as pyrimidines, pyridines, imidazoles and triazoles derivatives as well as bicyclic heterocycles such as quinazolines or quinoline derivatives (Figure 1 in green). These adenine mimics were coupled to the

cyclopentanediol moiety (Figure 1 in blue) linked to second substrate such as tert-butylaniline of Dia2 (Figure 1 in red). All compounds were screened using a combination of ligand-based virtual screening and molecular docking techniques (Supplementary Information).

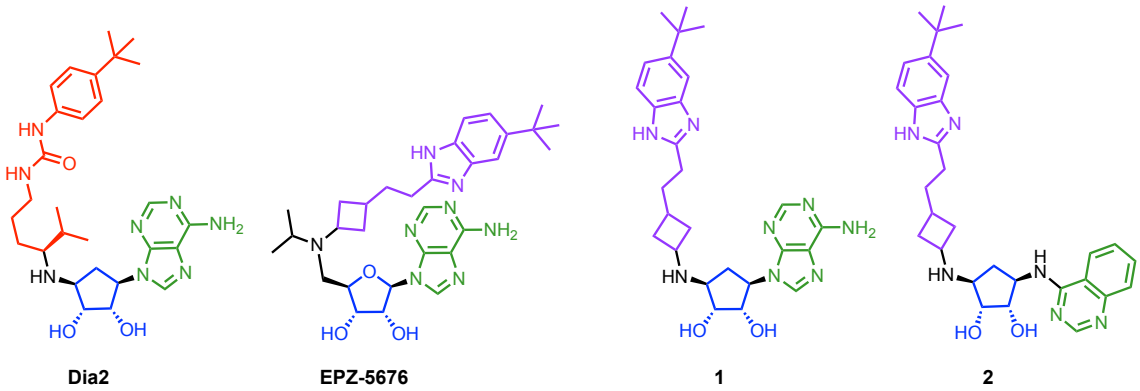

Figure 1- Chemical structure of compounds Dia2, EPZ-5676, and compounds **1** and **2**. In green is depicted the adenine and the quinazoline, in blue the ribose or the cyclopentane diol, and in red or violet the second substrate mimics.

The virtual screening of 50 compounds identified that the quinazoline moiety as the best adenine mimic among the explored heterocycles able to maintain a significant number of interactions with the adenosine pocket in the DOT1L protein. We thus chose it to replace the adenine in the bisubstrate inhibitor.

For the second moiety of the molecule, we chose the linker arm and substituent of the most potent inhibitor EPZ-5676 (in violet in Figure 1). Unfortunately, we never succeeded to synthesize a second substrate bearing the isopropyl moiety coupled to the cyclobutane moiety as in EPZ5676 (Figure 1). So, we simplified the linker and directly coupled the cyclobutane on the aminocyclopentane diol, even if it led to a shorter linker

and the loss of the isopropyl group. Consequently, compounds **1** and **(±)2** were synthesized to compare adenine and quinazoline moieties (in green in Figure 1).

2.2. Molecular docking of compounds 1 and 2

The molecular docking study was carried out on the 3D structure of DOT1L crystalized in complex with the EPZ-5676 inhibitor (PDB code: 4HRA). This was chosen because EZP5676 has the highest structural similarity to the designed compounds. The study was carried out using the GOLD 5.8.1 software.[38] Most interestingly, the adenylylcyclopentanediol moiety (compound **1**) and quinazolinylcyclopentadiol moiety (compound **2**) adopted binding modes similar to adenosine moiety of EPZ-5676 in the SAM binding pocket of DOT1L (Figure 2). The structure of EPZ-5676 co-crystalised with DOT1L shows that the inhibitor induces a hydrophobic sub-pocket occupied by the *t*-butylbenzimidazole moiety.[44] In the docking studies, the *t*-butylbenzimidazole moiety of compounds **1** and **2** occupied the same pocket.

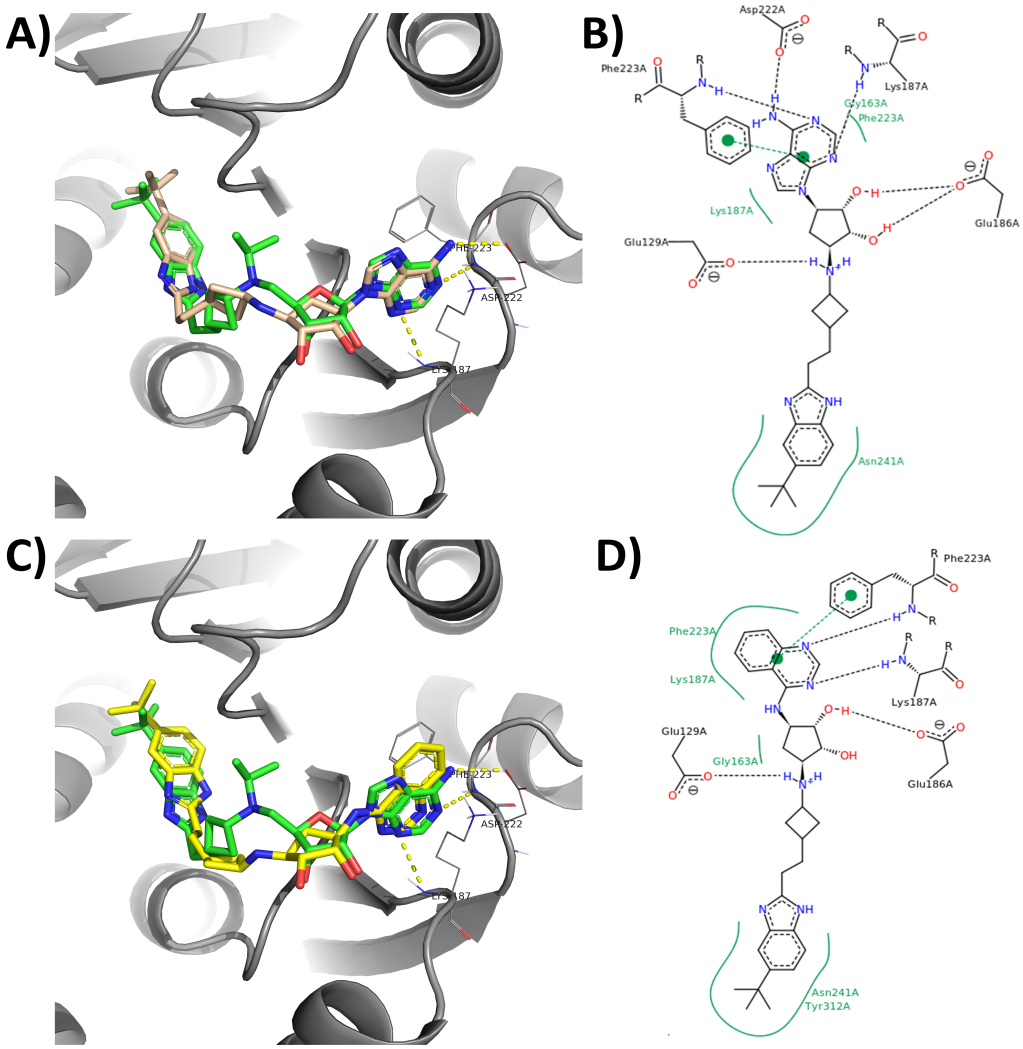

Figure 2- Predicted binding modes of compounds **1** and 3*S*,5*R* enantiomer of **2** obtained by molecular docking in the crystal structure of DOT1L with EPZ-5676 (PBD code: 4HRA). **A)** Comparison of binding modes of EPZ-5676 (green sticks) and compound **1** (yellow sticks) in the binding pocket of human DOT1L. Residues interacting with adenine moiety of the ligands are depicted in grey. The yellow hatches lines represent acceptor donor bond. **B)** 2D representation of the intermolecular interactions predicted for compound **1**. **C)** Comparison of binding modes of EPZ-5676 (green sticks) and compound **2** (yellow sticks) in the binding pocket of human DOT1L. **D)** 2D representation of the intermolecular interactions predicted for compound **2**.

The quinazoline moiety allowed very good interactions into the adenine pocket where the SAM substrate binds to DOT1L. Thus, the use of the quinazoline moiety kept intact the mode of binding as bisubstrate analogue [16].

To confirm the use of the quinazoline moiety as an adenine isostere, ~~we synthesized~~ compounds **1** and (±)-**2** were synthetised.

2.2. Chemical synthesis

Compound **1** was obtained by a one pot synthesis: reductive amination of **3** [45] and **4** [46] followed by deprotection of the isopropylidene moiety led to the desired compound **1** (Figure 3).

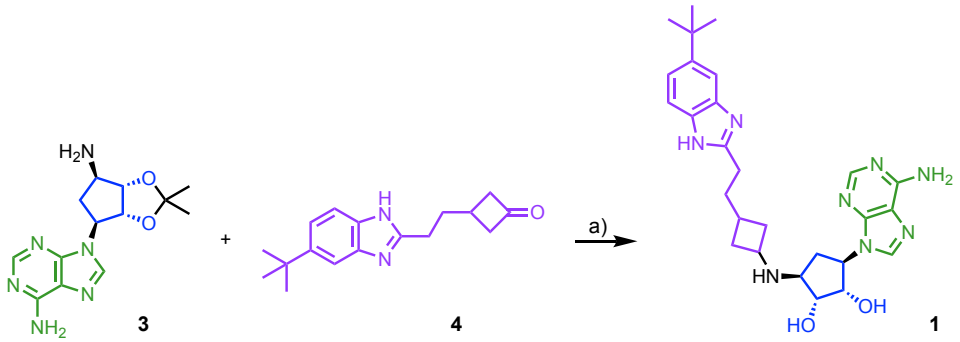

Figure 3- Synthesis of the adenine derivative **1.** a) *i.* $NaBH_3CN$, MeOH, RT, 12h; *ii.* TFA, H_2O, RT, 1h, 47% over two steps.

Compound **(±)-2**was synthesized with the same procedure from benzylimidazole **4** and amine **10** (Figure 4). Amine **10** was obtained as following: Boc protection of compounds **5** [47] was achieved to isolate compound **6** that was protected by acetalization to yield compound **7**. The selective deprotection of **7** in dry acidic media afforded **8** that was reacted with triazoloquinoline **9** to yield compound **10**.

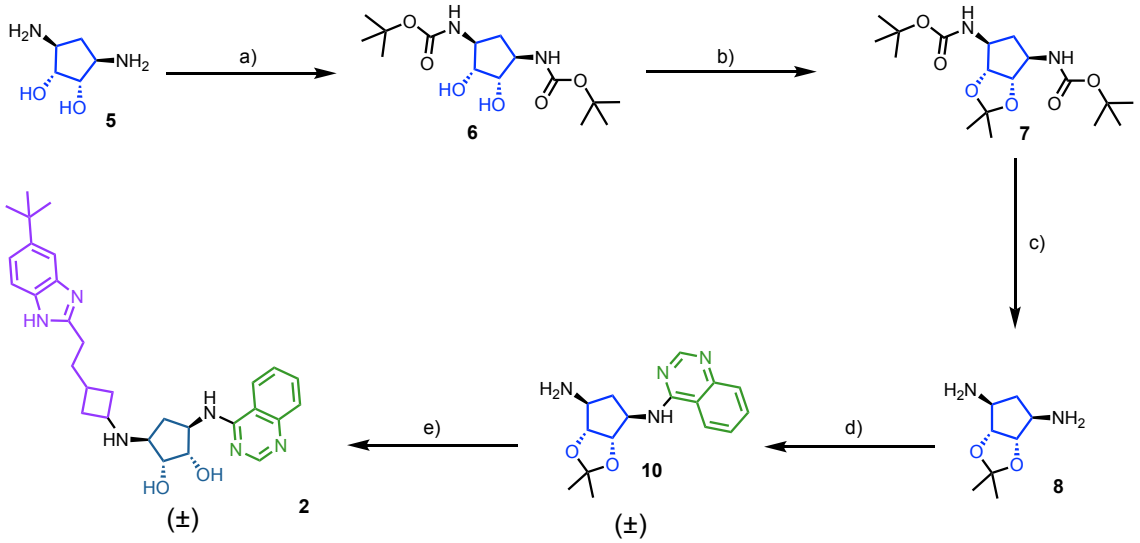

Figure 4- Synthesis of the quinazoline derivative **2**. a) Boc_2O, Et_3N, Dioxane : H_2O, RT, 16h, 95%. b) pTSA, acetone, RT, 12h, 96%. c) TFA, DCM, RT, 30min, 75%. d) **9**, Et_3N, ACN, RT, 12h, 74%. e) *i.* **4**, $NaBH_3CN$, MeOH, RT, 12h; *ii.* TFA, H_2O, RT, 1h, 38% over two steps.

2.3. Biological evaluation

Inhibition of the enzymatic activity of recombinant hDOT1L.

First, the ability of compounds **1** and **(±)-2** to inhibit DOT1L was evaluated in an *in vitro* AlphaLISA assay using recombinant catalytic hDOT1L and purified nucleosomes and compared to EPZ-5676 (Figure 5 and Table 1).

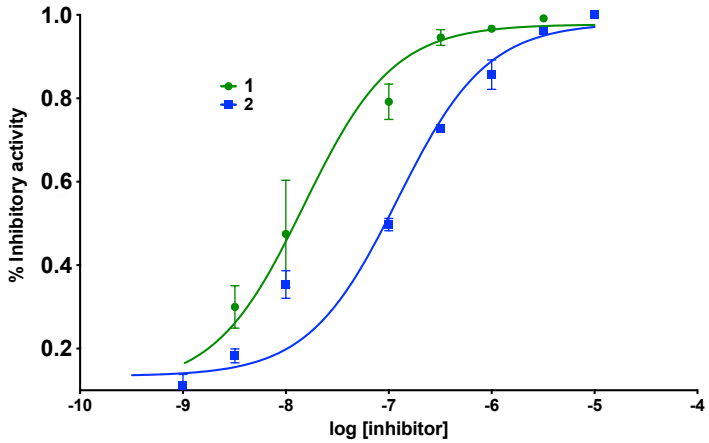

Figure 5- Inhibition of recombinant human DOT1L by compounds **1** (green) and **(±)-2** (blue). Each data point represents the mean of two technical replicates and two independent experiments.

Table 1. Obtained GoldScore values for docked ligands and inhibition of hDOT1L inhibitory activity expressed as IC_{50} (nM).

Compound	GoldScore	IC_{50} in nM
EPZ-5676	105.007	0.4 ± 0.1
1	92.840	30 ± 0.3
2	86.670	121 ± 2

Compound **1** appeared to be more active than **(±)-2** against the recombinant enzyme with an IC_{50} of 30nM and 121nM, respectively. Already in the parent compound Dia2 [26], the change in the attachment from a C5' carbon atom to a NH, gave a 10-fold loss activity. Here in addition, the linker to the second substrate is shorter by one carbon atom compared to EPZ-5676, which could explain an additional loss in activity. The scoring functions (GoldScore) from the docking reflected the inhibitory activities of the assayed compounds (Table 1). The experimental data corroborate the predicted binding modes.

The decrease in the inhibitory activity of compound **(±)-2** can be explained by the lack of additional hydrogen bonds with Asp222 in the SAM pocket of DOT1L (Figure 2). Indeed, the adenine moiety of compounds **1** and EPZ-5676 establishes three hydrogen bonding interactions: the 6-NH_2 of adenine with Asp222; the adenine N5 with Phe223 and the adenine N3 with Lys187 (Figure 2A and B); while the quinazoline moiety of compound **(±)-2** makes only two hydrogen bonds, with Phe223 and Lys187 (Figure 2C and D).

Since our main aim was to prove the feasibility of replacing the adenine moiety by an alternative group and since compound **(±)-2** maintained a nanomolar activity *in vitro* against DOT1L, we explored its activity in cellular assays in comparison to the adenine derivative **1**.

Inhibition of the proliferation of MLLr cells.

Both compounds **1** and **(±)-2** were tested for their ability to inhibit the proliferation of the MV4-11 cell line, derived from an MLLr patient with the MLL-AF4 translocation [48], as this cell line is known to be dependent on DOT1L[18].

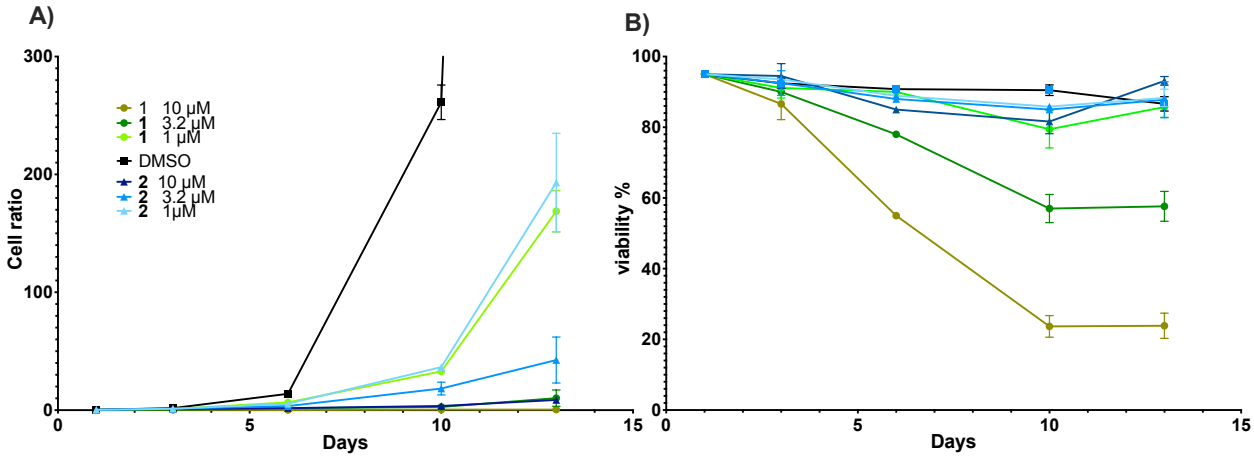

Figure 6. A) Cellular growth of MV4-11 (MLL-AF4) followed up to 13 days upon treatment with 10 µM (dark green curve), 3.2 µM (green curve), 1.0 µM (light green curve) of compound **1** and 10 µM (dark blue curve), 3.2 µM (blue curve), 1.0 µM (light blue curve) of compound **2**. Viable cells were counted every 3 to 4 days in the presence of **1**, **(±)-2** or DMSO (-) (black plain curve) and the ratio number of cells over initial population were plotted. **B)** Viability of MV4-11 (MLL-AF4) cells upon treatment with 10 µM (dark green curve), 3.2 µM (green curve), 1.0 µM (light green curve) of compound **1** and 10 µM (dark blue curve), 3.2 µM (blue curve), 1.0 µM (light blue curve) of compound **(±)-2**. Viability of cells was evaluated every 3 to 4 days in the presence of **1**, **(±)-2** or DMSO (+) (black plain curve). Every data point are the results of technical duplicates.

Viability and proliferation were monitored upon treatment of the MV4-11 cells with compounds **1** and **(±)-2**, while DMSO was used as negative control (figure 6). The delay observed in the response reflects the time required to completely reverse the aberrant expression of the MLL fusion target genes by inhibition of DOT1L as described in the literature. [26,49]. After 4 days, MV4- 11 cell viability decreased with compound **1** at the highest doses, showing a cytotoxic effect. In contrast, treatment with **(±)-2** affected cell proliferation as compound **1**, but without affecting cell viability. MV4-11

cells remained viable in the presence of compound **(±)-2**, but their growing curve was slowed. In agreement, we found that compound induced a 50% antiproliferative effect after 72h of treatment at 3.4 ±1.1μM, while compound **(±)-2** at 12.9±1.1μM. EPZ5676 showed a higher cytotoxicity in MV4-11 (Supplementary Figure S4, in agreement with previous reports[25,26,28].

Having established that **1** and **(±)-2** are potent inhibitors of DOT1L and inhibit MLLr cell proliferation, we explored the ability of these compounds to decrease the methylation of H3K79 in cells to confirm the DOT1L target in cells.

Inhibition of H3K79 dimethylation in cells.

Histone were extracted from MV4-11 cells treated 6 days with compounds **1** and **(±)-2** at four concentrations (10, 3.2, 1.0 and 0.32 μM). In agreement with the proliferation data, a little number of cells and thus of histones were collected and purified after 10μM treatment. The amount of H3K79me2 normalized to total H3 collected was evaluated by Western blotting (Figure 7). The compounds were efficient to inhibit the demethylation of H3K79 upon 6 days treatment in a dose-dependent manner.

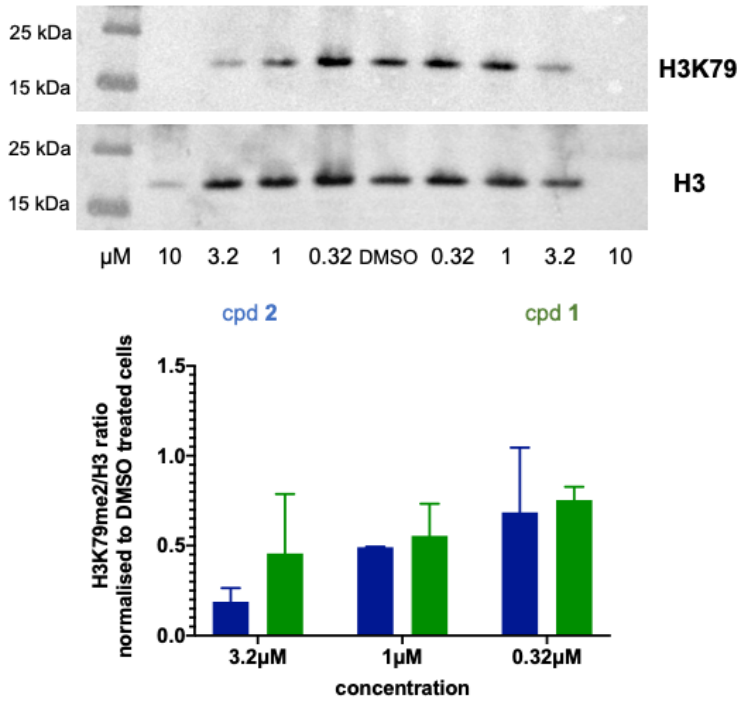

Figure 7- A representative Western blot of harvested histones from MV4-11 cells after 6 days treatment with compounds **1** (green) and **(±) 2** (blue) at 0.32, 1.0, 3.2, 10 µM) and quantification of two experiments of the H3K79me2 signal over the H3 signal normalised to cells treated with DMSO.

Effect on other histone marks in cells.

In order to quantify the effect of compounds on other histone marks in cells, we used a high-content screening assay developed in house (Supplementary figure S7). U2OS cells were exposed to the compounds at 1µM for 10 days and five histone marks levels (H3R2me2sy, H3R2me2asy, H3K9me1, H3K9me2, H3K79me2) were compared to non-treated cells using specific antibodies. Compounds **1** and **(±)-2** inhibited H3K79me2 in cells without affecting significantly the other tested histone marks.

Conclusions

We showed here that the replacement of the adenine moiety in a bisubstrate DOT-1-L inhibitor by a quinazoline moiety leads to slight loss in the inhibition of recombinant hDOT1L with an IC_{50} of 121nM. Interestingly, the quinazoline bisubstrate inhibitor **(±)-2** was less cytotoxic than the equivalent adenine analogue **1,** remaining at the same time

as potent at slowing down the proliferation of MLLr leukaemia cells and at inhibiting selectively H3K79 dimethylation in cells.

Moreover, the synthesis of analogues **1** and **(±)-2** and the experimental data comfort the virtual screening that we developed here.

Experimentally compound **(±)-2** was obtained as a mixture of two enantiomers, 1*S*,2*R*,3*S*,5*R* and 1*R*,2*S*,3*R*,5*S*. The molecular docking of the two enantiomers indicates that enantiomer 1*S*,2*R*,3*S*,5*R* showed a higher docking score compared to the 1*R*,2*S*,3*R*,5*S* stereoisomer (GoldScore=86.670 *vs.* GoldScore=83.468, Supplementary Figure S8), reflecting a potential higher affinity for DOT1L. Furthermore, while the 1*S*,2*R*,3*S*,5*R* enantiomer of **2** made interactions in the modelled SAM binding site of DOT1L in a pattern similar as EPZ-5676 and compound **1** (Figure 2), the molecular docking studies showed that the 1*R*,2*S*,3*R*,5*S* enantiomer of **(±)-2** does not fit correctly in the catalytic pocket (Supplementary Figure S8). The optimisation of a new chemical pathway leading to selective enantiomers is under study to obtain more potent compounds.

Finally, further extension of the use of the quinazoline moiety in the design of bisubstrate inhibitors of HMTs is ongoing in our laboratory to probe its capability to replace adenine. To replace the adenine, other heterocycles will also be studied and inserted in bisubstrate scaffolds.

Summary Points

- Synthesis of a cyclopentane derivative bearing a quinazoline analogue to mimic adenine
- This replacement allows a similar mode of action as the adenine parent compound
- Identification of a new chemical scaffold for DOT1L inhibition

- Development and experimental validation of a docking model for evaluation of the replacement of adenine in bisubstrate inhibitors
- The quinazoline moiety induces a reduced cytotoxicity in cells
- Both compounds block proliferation in MV4-11 cells
- Both compounds lower H3K79 methylation in cells

Funding: Région Ile de France supported the research with a Ph.D. fellowship to CB (ARDoC) and DIM OneHealth Investissements to PBA. Le Comité de Paris de la Ligue contre la Cancer (project Epi-Med 2020-2021) to PBA. Hubert Curien Partnership Project for collaboration France-Serbia 2020-2022 (Program Pavle Savic 2020) to PBA and KN.

The authors collaborated in the frame of the EU COST CM1406 Epigenetic Chemical Biology program.

DR, NDj and KN acknowledge project of Ministry of Science and Technological Development of the Republic of Serbia, Faculty of Pharmacy, Contract No. 451-03-9/2021-14/200161.

Acknowledgments: We thank Bruno Vitorge from the Institut Pasteur Biological NMR Technological Platform for helping with NMR experiments,
Frédéric Bonhomme and Sophie Vichier-Guerre of the CNRS-Institut Pasteur UMR3523 Organic Chemistry Unit for assisting with HRMS analysis.
We thank Image Analysis HUB at Institute Pasteur (Jean-Yves Tinevez, Stephane Rigaud, Dmitry Ershov, Minh Son Phan) for the help with analysis of images acquired by confocal microscope.

Author Contributions: All authors agreed on the manuscript content
Conflicts of Interest: The authors declare no conflict of interest

References

1. Choudhuri S. From Waddington's epigenetic landscape to small noncoding RNA: some important milestones in the history of epigenetics research. *Toxicol. Mech. Methods*. 21(4), 252–274 (2011).

2. Berger SL, Kouzarides T, Shiekhattar R, Shilatifard A. An operational definition of epigenetics. *Genes Dev.* 23(7), 781–783 (2009).

3. Goldberg AD, Allis CD, Bernstein E. Epigenetics: A Landscape Takes Shape. *Cell*. 128(4), 635–638 (2007).

4. Arimondo PB, Barberousse A, Pontarotti G. The Many Faces of Epigenetics Oxford, December 2017. *Epigenetics*. 14(6), 623–631 (2019).

5. Berger SL, Kouzarides T, Shiekhattar R, Shilatifard A. An operational definition of epigenetics. *Genes Dev.* 23(7), 781–783 (2009).

6. Ballestar E, Esteller M. The Epigenetic Breakdown of Cancer Cells: From DNA Methylation to Histone Modifications. In: *Epigenetics and Chromatin*. Jeanteur P (Ed.), Springer, Berlin, Heidelberg, 169–181 (2005)

7. Martin C, Zhang Y. The diverse functions of histone lysine methylation. *Nat. Rev. Mol. Cell Biol.* 6(11), 838–849 (2005).

8. Zhang Y, Reinberg D. Transcription regulation by histone methylation: interplay between different covalent modifications of the core histone tails. *Genes Dev.* 15(18), 2343–2360 (2001).

9. Santos-Rosa H, Schneider R, Bannister AJ, *et al.* Active genes are tri-methylated at K4 of histone H3. *Nature*. 419(6905), 407–411 (2002).

10. Greer EL, Shi Y. Histone methylation: a dynamic mark in health, disease and inheritance. *Nat. Rev. Genet.* 13(5), 343–357 (2012).

11. Feinberg AP, Oshimura M, Barrett JC. Epigenetic Mechanisms in Human Disease. *Cancer Res.* 62(22), 6784–6787 (2002).

12. Neganova ME, Klochkov SG, Aleksandrova YR, Aliev G. Histone modifications in epigenetic regulation of cancer: Perspectives and achieved progress. *Semin. Cancer Biol.* [Internet]. (2020).

13. Italiano A, Soria J-C, Toulmonde M, *et al.* Tazemetostat, an EZH2 inhibitor, in relapsed or refractory B-cell non-Hodgkin lymphoma and advanced solid tumours: a first-in-human, open-label, phase 1 study. *Lancet Oncol.* 19(5), 649–659 (2018).

14. Morschhauser F, Tilly H, Chaidos A, *et al.* Tazemetostat for patients with relapsed or refractory follicular lymphoma: an open-label, single-arm, multicentre, phase 2 trial. *Lancet Oncol.* 21(11), 1433–1442 (2020).

15. Hoy SM. Tazemetostat: First Approval. *Drugs*. 80(5), 513–521 (2020).

16. Bon C, Halby L, Arimondo PB. Bisubstrate inhibitors: the promise of a selective and potent chemical inhibition of epigenetic 'writers.' *Epigenomics*

17. Chen Y, Zhu W-G. Biological function and regulation of histone and non-histone lysine methylation in response to DNA damage. *Acta Biochim. Biophys. Sin.* 48(7), 603–616 (2016).

18. Bon C, Si Y, Arimondo PB. Chapter 4 - Targeting DOT1L for mixed-lineage rearranged leukemia [Internet]. In: *Histone Modifications in Therapy*. Castelo-Branco P, Jeronimo C (Eds.), Academic Press, 81–99 (2020)

19. Wu F, Nie S, Yao Y, *et al.* Small-molecule inhibitor of AF9/ENL-DOT1L/AF4/AFF4 interactions suppresses malignant gene expression and tumor growth. *Theranostics*. 11(17), 8172–8184 (2021).

20. Grigsby SM, Friedman A, Chase J, *et al.* Elucidating the Importance of DOT1L Recruitment in MLL-AF9 Leukemia and Hematopoiesis. *Cancers*. 13(4), 642 (2021).

21. Sarno F, Nebbioso A, Altucci L. DOT1L: a key target in normal chromatin remodelling and in mixed-lineage leukaemia treatment. *Epigenetics*. 15(5), 439–453

(2020).

22. Bernt KM, Zhu N, Sinha AU, *et al.* MLL-Rearranged Leukemia Is Dependent on Aberrant H3K79 Methylation by DOT1L. *Cancer Cell*. 20(1), 66–78 (2011).

23. Perner F, Gadrey JY, Xiong Y, *et al.* Novel inhibitors of the histone methyltransferase DOT1L show potent antileukemic activity in patient-derived xenografts. *Blood*. 136(17), 1983–1988 (2020).**

24. Lonetti A, Indio V, Laginestra MA, *et al.* Inhibition of Methyltransferase DOT1L Sensitizes to Sorafenib Treatment AML Cells Irrespective of MLL-Rearrangements: A Novel Therapeutic Strategy for Pediatric AML. *Cancers*. 12(7), 1972 (2020).

25. Daigle SR, Olhava EJ, Therkelsen CA, *et al.* Selective killing of mixed lineage leukemia cells by a potent small-molecule DOT1L inhibitor. *Cancer Cell*. 20(1), 53–65 (2011).**

26. Bon C, Si Y, Pernak M, *et al.* Synthesis and Biological Activity of a Cytostatic Inhibitor of MLLr Leukemia Targeting the DOT1L Protein. *Molecules*. 26(17), 5300 (2021).**

27. Shukla N, Wetmore C, O'Brien MM, *et al.* Final Report of Phase 1 Study of the DOT1L Inhibitor, Pinometostat (EPZ-5676), in Children with Relapsed or Refractory MLL-r Acute Leukemia. *Blood*. 128(22), 2780–2780 (2016).

28. Basavapathruni A, Olhava EJ, Daigle SR, *et al.* Nonclinical pharmacokinetics and metabolism of EPZ-5676, a novel DOT1L histone methyltransferase inhibitor. *Biopharm. Drug Dispos.* 35(4), 237–252 (2014).*

29. Stauffer F, Weiss A, Scheufler C, *et al.* New Potent DOT1L Inhibitors for in Vivo Evaluation in Mouse. *ACS Med. Chem. Lett.* 10(12), 1655–1660 (2019).*

30. Chen C, Zhu H, Stauffer F, *et al.* Discovery of Novel Dot1L Inhibitors through a

Structure-Based Fragmentation Approach. *ACS Med. Chem. Lett.* 7(8), 735–740 (2016).*

31. Möbitz H, Machauer R, Holzer P, *et al.* Discovery of Potent, Selective, and Structurally Novel Dot1L Inhibitors by a Fragment Linking Approach. *ACS Med. Chem. Lett.* 8(3), 338–343 (2017).*

32. Gibbons GS, Chakraborty A, Grigsby SM, *et al.* Identification of DOT1L inhibitors by structure-based virtual screening adapted from a nucleoside-focused library. *Eur. J. Med. Chem.* 189, 112023 (2020).*

33. Pasco M, Moumné R, Lecourt T, Micouin L. Stereoselective Synthesis of Fluorinated 1,3-cis-Diaminocyclopentanes. *J. Org. Chem.* 76(12), 5137–5142 (2011).

34. Olhava EJ. Methods of Synthesizing Substituted Purine Compounds [Internet]. (US201361799147P 20130315) (2014).

35. Martínez-Rosell G, Giorgino T, De Fabritiis G. PlayMolecule ProteinPrepare: A Web Application for Protein Preparation for Molecular Dynamics Simulations. *J. Chem. Inf. Model.* 57(7), 1511–1516 (2017).

36. Frisch MJ, Head-Gordon M, Trucks GW, *et al.* Gaussian 90. Gaussian, Inc., Pittsburgh, PA.

37. ChemBio3D Ultra. Corporation, C.

38. Jones G, Willett P, Glen RC, Leach AR, Taylor R. Development and validation of a genetic algorithm for flexible docking11Edited by F. E. Cohen. *J. Mol. Biol.* 267(3), 727–748 (1997).

39. The Open-Source PyMOL Molecular Graphics System 1.7.x. Schrödinger, LLC.

40. Stierand K, Rarey M. PoseView -- molecular interaction patterns at a glance. *J. Cheminformatics*. 2(1), P50 (2010).

41. Basavapathruni A, Olhava EJ, Daigle SR, *et al.* Nonclinical pharmacokinetics

and metabolism of EPZ-5676, a novel DOT1L histone methyltransferase inhibitor. *Biopharm. Drug Dispos.* 35(4), 237–252 (2014).

42. Campbell CT, Haladyna JN, Drubin DA, *et al.* Mechanisms of Pinometostat (EPZ-5676) Treatment–Emergent Resistance in MLL-Rearranged Leukemia. *Mol. Cancer Ther.* 16(8), 1669–1679 (2017).

43. Daigle SR, Olhava EJ, Therkelsen CA, *et al.* Potent inhibition of DOT1L as treatment of MLL-fusion leukemia. *Blood*. 122(6), 1017–1025 (2013).**

44. Basavapathruni A, Jin L, Daigle SR, *et al.* Conformational Adaptation Drives Potent, Selective and Durable Inhibition of the Human Protein Methyltransferase DOT1L. *Chem. Biol. Drug Des.* 80(6), 971–980 (2012).*

45. Hegde VR, Seley KL, Schneller SW, Elder TJJ. 5‘-Amino-5‘-deoxy-5‘-noraristeromycin. *J. Org. Chem.* 63(20), 7092–7094 (1998).

46. Olhava EJ, Chesworth R, Kuntz KW, Richon VM, Pollock RM, Daigle SR. Substituted Purine and 7 - Deazapurine Compounds as Modulators of Epigenetic Enzymes [Internet]. (US20100419661P 20101203) (2012).

47. Pasco M, Moumné R, Lecourt T, Micouin L. Stereoselective Synthesis of Fluorinated 1,3-cis-Diaminocyclopentanes. *J. Org. Chem.* 76(12), 5137–5142 (2011).

48. Prange KHM, Mandoli A, Kuznetsova T, *et al.* MLL-AF9 and MLL-AF4 oncofusion proteins bind a distinct enhancer repertoire and target the RUNX1 program in 11q23 acute myeloid leukemia. *Oncogene*. 36(23), 3346–3356 (2017).

49. Jones B, Su H, Bhat A, *et al.* The histone H3K79 methyltransferase Dot1L is essential for mammalian development and heterochromatin structure. *PLoS Genet.* 4(9), e1000190 (2008).